

# Efimov physics in bosonic atom-trimer scattering

A. Deltuva

*Centro de Física Nuclear da Universidade de Lisboa, P-1649-003 Lisboa, Portugal*

(Received August 10, 2010)

Bosonic atom-trimer scattering is studied in the unitary limit using momentum-space equations for four-particle transition operators. The impact of the Efimov effect on the atom-trimer scattering observables is explored and a number of universal relations is established. Positions and widths of tetramer resonances are determined. Trimer relaxation rate constant is calculated.

PACS numbers: 31.15.ac, 34.50.-s, 34.50.Cx

Few-particle systems with resonant interactions, characterized by the two-particle scattering length  $a$  being much larger than the range of the interaction, were predicted to have a number of universal (interaction-independent) properties and correlations between observables [1–6]. Such a behavior was recently confirmed in cold atom physics experiments [7, 8], but can be seen qualitatively also in few-nucleon systems [1, 2]. One of the best-known examples is the existence of the infinite number of weakly bound three-boson states (Efimov trimers) in the unitary limit  $a = \infty$  [1]. In that limit, depending on the available energy, an infinite number of atom-trimer channels may be present in the four-boson system. Due to complexity of the multichannel four-particle scattering problem the universal properties of such a system, i.e., the atom-trimer continuum, are not known yet; we therefore aim to study them for the first time in the present work. Furthermore, the existence of a pair of four-boson states (tetramers) associated with each Efimov trimer was predicted [3, 5]. However, only the two tetramers associated with the trimer ground state are true bound states that have been studied in all the details using standard bound state techniques [3–5, 9]. Higher tetramers are resonances above the atom-trimer threshold and for this reason their properties are far less known; they will be determined in the present work using proper scattering calculations.

Our description of the four-boson scattering is based on the Alt, Grassberger and Sandhas (AGS) equations [10] for the transition operators; they are equivalent to the Faddeev-Yakubovsky equations [11] for the wavefunction components. Symmetrized form of AGS equations [12] is appropriate for the system of four identical bosons,

$$\mathcal{U}_{11} = P_{34}(G_0 t G_0)^{-1} + P_{34}U_1 G_0 t G_0 \mathcal{U}_{11} + U_2 G_0 t G_0 \mathcal{U}_{21}, \quad (1a)$$

$$\mathcal{U}_{21} = (1 + P_{34})(G_0 t G_0)^{-1} + (1 + P_{34})U_1 G_0 t G_0 \mathcal{U}_{11}, \quad (1b)$$

where  $\mathcal{U}_{\beta\alpha}$  are the four-particle transition operators,  $G_0$  is the four free particle Green's function, and  $P_{34}$  is the permutation operator of particles 3 and 4 that ensures correct permutation symmetry of the system. The dynamic input is the two-boson potential  $v$  from which the two-particle transition-matrix  $t$  and the AGS transition

operators  $U_\alpha$  are derived, with  $\alpha = 1$  and  $2$  corresponding to the  $1 + 3$  and  $2 + 2$  subsystems, respectively. As explained in Ref. [12], the atom-trimer scattering amplitudes are given by the on-shell matrix elements of  $\mathcal{U}_{11}$  calculated between the Faddeev amplitudes of the corresponding initial and final states.

We solve AGS equations using momentum-space partial-wave representation [12] where they are a system of coupled three-variable integral equations that after the discretization of momentum variables becomes a very large system of linear algebraic equations. In the case of the four-nucleon scattering those equations have been successfully solved with realistic nuclear and Coulomb interactions [13, 14]. In the present calculations we take the numerical techniques for the treatment of four-particle permutations and trimer bound-state poles from Refs. [12–14]. However, an important difference as compared to the four-nucleon system is the presence of sharp resonances in the four-boson system, manifesting themselves as poles of the AGS operators (1). Since the convergence of the multiple scattering series in the vicinity of the pole is very slow, in this work we solve systems of linear equations by the direct matrix inversion instead of the iterative double Padé summation method [12]. Since we are interested in the universal properties that must be independent of the interaction details, we use rank 1 separable two-boson potentials  $v = |g\rangle\lambda\langle g|$  acting in  $S$ -wave only and thereby reducing Eqs. (1) to a small system of two-variable integral equations. Although the two-boson interaction is limited to  $S$ -wave, i.e.,  $l_x = 0$  in the notation of Ref. [12], higher angular momentum states with  $l_y, l_z \leq 2$  have to be taken into account for the relative motion in  $1 + 2$ ,  $1 + 3$ , and  $2 + 2$  subsystems to achieve the convergence.

Our standard potential has simple gaussian form factor, i.e., its momentum-dependence is  $\langle k|g\rangle = e^{-(k/\Lambda)^2}$ . The strength  $\lambda$  is chosen to reproduce infinite two-boson scattering length. In that limit all observables scale with  $\Lambda$ ; e.g., the binding energy of the  $n$ -th excited trimer  $b_n \sim \Lambda^2$ . It therefore makes no sense to specify particular value of  $\Lambda$  as well as boson mass. Instead, we will use dimensionless ratios. As the length scale associated with the  $n$ -th excited trimer we will use  $l_n = \hbar/\sqrt{2\mu_1 b_n}$  where  $\mu_1$  is the reduced atom-trimer mass.

We do not include explicit three-body force, however, many-body forces are simulated by a different off-shell

| $n$ | $b_{n-1}/b_n$ | $\kappa_{n-1}/\kappa_n$ | $b_n/\kappa_n$        |
|-----|---------------|-------------------------|-----------------------|
| 1   | 548.114       | 32.734                  | $1.03 \times 10^{-2}$ |
| 2   | 515.214       | 23.697                  | $4.73 \times 10^{-4}$ |
| 3   | 515.036       | 22.767                  | $2.09 \times 10^{-5}$ |
| 4   | 515.035       | 22.699                  | $9.22 \times 10^{-7}$ |
| 5   | 515.035       | 22.695                  | $4.06 \times 10^{-8}$ |
| 1   | 2126.36       | 11.349                  | $2.14 \times 10^{-3}$ |
| 2   | 518.570       | 21.528                  | $8.87 \times 10^{-5}$ |
| 3   | 515.042       | 22.655                  | $3.90 \times 10^{-6}$ |
| 4   | 515.035       | 22.694                  | $1.72 \times 10^{-7}$ |

TABLE I. Trimer properties obtained with one-term (top) and two-term form factor potentials (bottom).

behavior of the two-body potential. To prove that this doesn't change universal properties of the four-boson system we also use the potential II with two-term form factor  $\langle k|g\rangle = [1 + c_2 (k/\Lambda)^2]e^{-(k/\Lambda)^2}$ ; large negative value of  $c_2 = -9.17$  ensures very different off-shell behavior. In the configuration space representation the potential II has several attractive and repulsive regions much like the one of Ref. [15] and supports a deeply bound trimer that is non Efimov state in contrast to excited states and all states of the standard potential. This can be seen in Table I which collects ratios for calculated trimer binding energies  $b_n$ : all  $b_{n-1}/b_n$  are quite close to the characteristic Efimov value of 515.035, the exception being  $b_0/b_1$  for the potential II that is much larger. However, the Efimov value is reached with good accuracy only for high excited states  $n \geq 3$ . This is not surprising since the Efimov condition  $R_n \gg \rho$  ensuring truly universal behavior, where  $R_n$  is the size of the  $n$ -th trimer and  $\rho$  the range of the interaction, is only well satisfied for  $n$  large enough whereas for the ground states  $R_0 < \rho$  may take place [15, 16]. Simultaneously  $\kappa_{n-1}/\kappa_n$  converges towards 22.694 where  $\kappa_n$  is the expectation value of the  $n$ -th excited trimer internal kinetic energy. The ratio  $b_n/\kappa_n$  is a measure for the high-momentum components in the trimer wave function; as Table I demonstrates, it differs significantly for the two employed potentials.

In Table II we present results for the scattering length  $a_n$  and effective range  $r_n$  for the atom scattering from the  $n$ -th excited trimer up to  $n = 5$ . For both potentials  $a_n/l_n$  and  $r_n/l_n$  converge towards universal values as  $n$  increases, i.e.,

$$a_n/l_n \approx 22.6 - 1.09i, \quad (2a)$$

$$r_n/l_n \approx 3.22 - 0.017i, \quad (2b)$$

however, significant potential-dependent deviations are observed for  $n \leq 2$ . Including strong repulsive three-body force that enforces the Efimov condition  $R_n \gg \rho$  (but with additional numerical complications) probably could speedup the convergence with  $n$  but even in such a case  $n = 0$  would be insufficient since it doesn't account for inelasticities.

| $n$ | $\text{Re}(a_n)/l_n$ | $\text{Im}(a_n)/l_n$ | $\text{Re}(r_n)/l_n$ | $\text{Im}(r_n)/l_n$ |
|-----|----------------------|----------------------|----------------------|----------------------|
| 1   | 31.1                 | -5.18                | 3.35                 | -0.043               |
| 2   | 23.1                 | -1.05                | 3.23                 | -0.016               |
| 3   | 22.7                 | -1.08                | 3.22                 | -0.017               |
| 4   | 22.6                 | -1.09                | 3.22                 | -0.017               |
| 5   | 22.6                 | -1.09                | 3.22                 | -0.017               |
| 1   | 11.7                 | -0.21                | 2.93                 | -0.012               |
| 2   | 22.5                 | -1.52                | 3.22                 | -0.024               |
| 3   | 22.7                 | -1.09                | 3.22                 | -0.017               |
| 4   | 22.6                 | -1.09                | 3.22                 | -0.017               |

TABLE II. Atom-trimer scattering length and effective range obtained with one-term (top) and two-term form factor potentials (bottom).

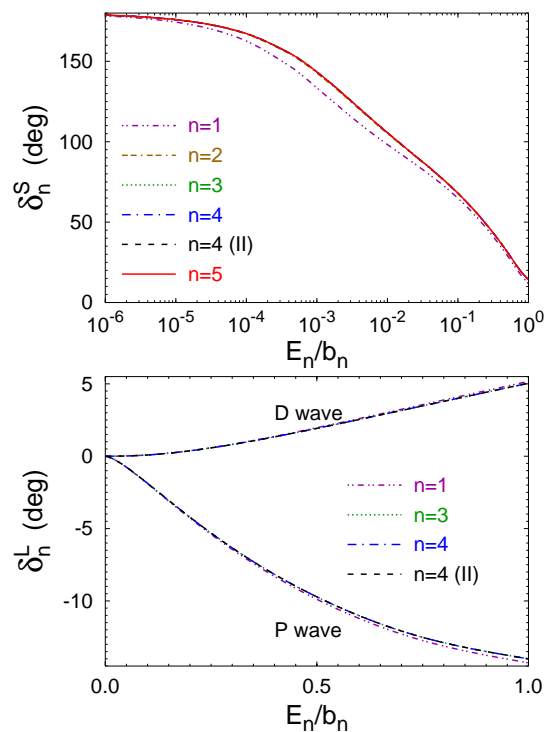


FIG. 1. (Color online)  $S$ -,  $P$ - and  $D$ -wave phase shift for the atom scattering from the  $n$ -th excited trimer.

It turns out that the universal limit exists for all scattering observables. In Figs. 1 - 2 we show all relevant phase shifts  $\delta_n^L$  and  $S$ -wave inelasticity parameter  $\eta_n^S$  for the atom scattering from the  $n$ -th excited trimer as functions of the relative kinetic energy  $E_n$  divided by the respective  $b_n$ ; the elastic  $S$ -matrix is parametrized as  $s_n^L = \eta_n^L e^{2i\delta_n^L}$ . Again, results with  $n \geq 3$  are indistinguishable and represent the universal values, but deviations are seen for lower  $n$ . Elastic scattering is determined by relative atom-trimer  $S$ -,  $P$ -, and  $D$ -waves. In fact,  $S$ -wave dominates at lower energies but close to  $E_n/b_n = 1$  the individual contributions of  $S$ -,  $P$ -, and

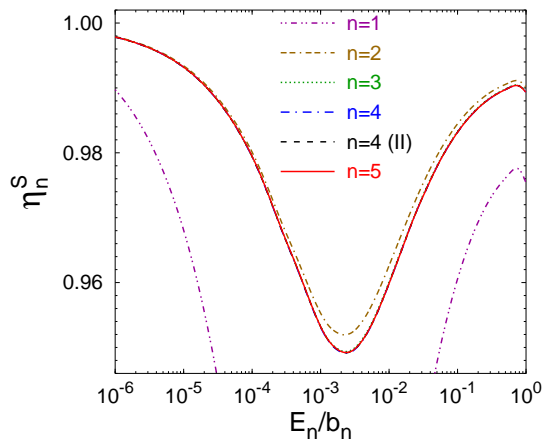


FIG. 2. (Color online)  $S$ -wave inelasticity parameter for the atom scattering from the  $n$ -th excited trimer.

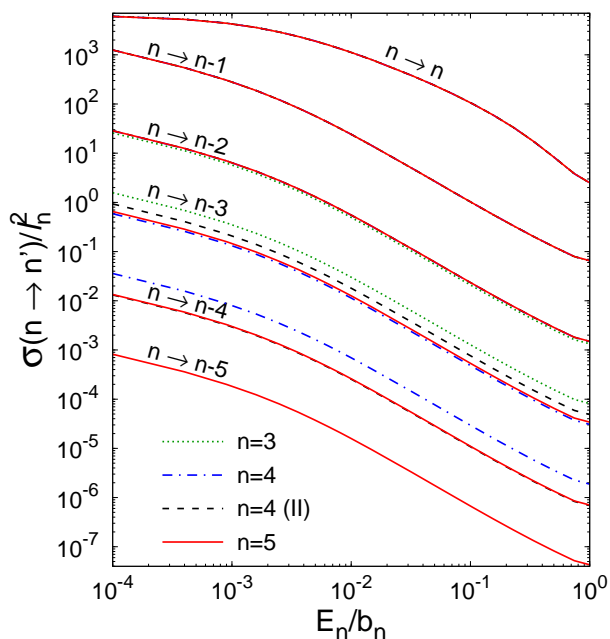


FIG. 3. (Color online) Elastic and inelastic cross sections for the atom scattering from the  $n$ -th excited trimer.

$D$ -waves to the elastic cross section are 31, 58, an 11%, respectively, while the  $F$ -wave with  $|\delta_n^F| < 0.4^\circ$  yields less than 0.1% and therefore is negligible. Situation is different in the inelastic scattering where only  $S$ -wave contributes significantly: only  $\eta_n^S$  clearly deviates from 1 as shown in Fig. 2 while in higher partial waves, due to very different size of trimers and the angular momentum barrier, transitions to other trimers are strongly suppressed and  $\eta_n^L$  are very close to 1, e.g.,  $1 - \eta_n^P < 10^{-6}$ .

The elastic and inelastic cross sections  $\sigma(n \rightarrow n')$  for the atom scattering from the  $n$ -th excited trimer leading to the lower-lying  $n'$ -th trimer are presented in Fig. 3. We do not show cross sections for  $n < n'$  that can be obtained by time reversal as  $\sigma(n' \rightarrow n) = (E_n/E_{n'})\sigma(n \rightarrow n')$ .

Within the resolution of the plot  $\sigma(n \rightarrow n')/l_n^2$  for  $n, n' \geq 2$  and fixed  $n - n'$  are independent of  $n$  and employed potential and thereby represent the universal values. Furthermore, for  $n > n'$  large enough the ratios

$$\frac{\sigma(n \rightarrow n')}{\sigma(n \rightarrow n' - 1)} \approx 43.7 \quad (3)$$

are energy-independent. These observations allow us to extrapolate  $\sigma(n \rightarrow n')$  results to any  $n$  and  $n'$  that are sufficiently large.

Perhaps most interesting energy regions, namely those containing  $S$ -wave four-boson resonances just slightly below  $E_n/b_n = 1$ , are not displayed in Fig. 3. There are two ( $k = 1, 2$ ) four-boson resonances associated with the  $N$ -th Efimov trimer. Resonances are poles of the AGS transition operators in the complex plane; thus, in the vicinity of the four-boson resonance

$$\mathcal{U}_{\beta\alpha} \approx \hat{\mathcal{U}}_{\beta\alpha}^{(-1)}(E - E_r)^{-1} + \hat{\mathcal{U}}_{\beta\alpha}^{(0)} + \hat{\mathcal{U}}_{\beta\alpha}^{(1)}(E - E_r), \quad (4)$$

where  $E = E_n - b_n$  and  $E_r = -B_{N,k} - i\Gamma_{N,k}/2$  with  $-B_{N,k}$  being the  $(N, k)$ -th resonance position relative to the four-body breakup threshold and  $\Gamma_{N,k}$  its width. These parameters were determined by fitting the on-shell matrix elements of  $\mathcal{U}_{11}$  into Eq. (4). Again, for  $N$  large enough, i.e.,  $N \geq 3$ , the results with good accuracy become independent of potential and  $N$ ,

$$B_{N,1}/b_N \approx 4.6108, \quad \Gamma_{N,1}/2b_N \approx 0.01484, \quad (5a)$$

$$B_{N,2}/b_N \approx 1.00228, \quad \Gamma_{N,2}/2b_N \approx 2.38 \times 10^{-4}. \quad (5b)$$

We note that  $B_{N,k}$  but not  $\Gamma_{N,k}$  have already been calculated in Ref. [5]. While  $B_{N,1}/b_N \approx 4.58$  of Ref. [5] is quite close to our number, the  $k = 2$  resonance with  $B_{N,2}/b_N \approx 1.01$  was predicted in Ref. [5] to be significantly further from the atom-trimer threshold than our result. In contrast to  $S$ -wave, there is no four-boson resonances in higher angular momentum states as can be seen in the bottom panel of Fig. 1.

Unlike in nuclear physics, the direct measurement of the atom-trimer cross sections in cold atom physics experiments is not possible yet. Instead, one may be able to create an ultracold mixture of atoms and excited Efimov trimers in a trap and observe the trimer relaxation, i.e., the inelastic collision of an atom and trimer in the  $n$ -th excited state leading to the atom and trimer in the lower-lying  $n'$ -th state. The kinetic energy  $\Delta K \approx b_{n'}$  released in this process is shared between the atom and trimer with the ratio 3:1. Thus, if  $b_{n'}/4$  is larger than trapping potential, the final-state trimer escapes the trap. Assuming that this is the dominating mechanism for the trimer loss, the time evolution of the density  $\rho_n(t)$  of the  $n$ -th excited state trimers in the trap is given by

$$\frac{d\rho_n(t)}{dt} = -\beta_n \rho_a(t) \rho_n(t), \quad (6)$$

$\rho_a(t)$  being the atom density and  $\beta_n$  the relaxation rate constant [2]. The alternative way of the trimer loss,

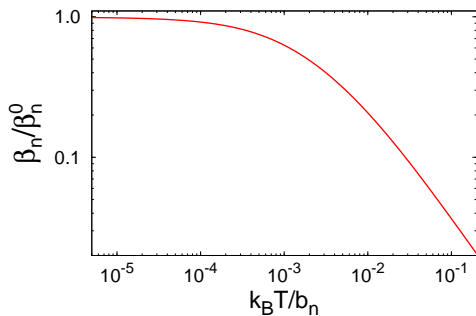


FIG. 4. (Color online) Temperature dependence of the trimer relaxation rate constant.

i.e., inelastic trimer-trimer collisions, is suppressed if  $\rho_n(0) \ll \rho_a(0)$ . Under this condition  $\rho_a(t) \approx \rho_a(0)$  and Eq. (6) has a simple solution

$$\rho_n(t) = \rho_n(0)e^{-\beta_n \rho_a(0)t}. \quad (7)$$

Thus, in this case the lifetime of the mixture is simply given by  $1/\beta_n \rho_a(0)$ . The relaxation rate constant  $\beta_n = \sum_{n'} \beta_{n \rightarrow n'}$  has contributions  $\beta_{n \rightarrow n'} = \langle v_n \sigma(n \rightarrow n') \rangle$  from transitions to all trimers  $n' < n$ , where  $v_n = \sqrt{2E_n/\mu_1}$  is the relative atom-trimer velocity and  $\langle \dots \rangle$  denotes the thermal average. Thus, the trimer relaxation rate constant is determined by the atom-trimer inelastic cross sections calculated in the present work. In particular, Eq. (3) implies that for  $n$  and  $n'$  large enough  $\beta_{n \rightarrow n'}/\beta_{n \rightarrow n'-1} \approx 43.7$  and therefore the relaxation is strongly dominated by the  $n \rightarrow n-1$  transition. The zero temperature limit of the relaxation rate constant can be obtained using the optical theorem as

$$\beta_n^0 = -\frac{4\pi\hbar}{\mu_1} \text{Im}(a_n). \quad (8)$$

The results at finite temperature  $T$  are given in Fig. 4 as-

suming the Boltzmann distribution for the relative atom-trimer energy;  $k_B$  is the Boltzmann constant. Figure 4 indicates that the use of  $T = 0$  limit is inappropriate at temperatures above  $k_B T/b_n > 10^{-4}$ .

In summary, we studied bosonic atom-trimer scattering in the unitary limit. It is a complicated multichannel four-particle scattering problem involving, in the present calculations, up to six open channels with the Efimov trimer binding energies differing by a factor larger than  $515^5 \approx 4 \times 10^{13}$ . Exact AGS equations were solved in momentum-space framework with some important technical modifications compared to previous calculations of the four-nucleon system. The results for reactions with highly excited trimers (at least 2nd excited state) in the initial and final channels were found to be independent of the used potential and thereby represent universal values for atom-trimer scattering length, effective range, phase shifts, elastic and inelastic cross sections and four-boson resonance parameters. On the other hand, results for lower trimers demonstrate that significant quantitative deviations from the universal behavior are possible. The comparison with the experimental data could not be performed yet, but the obtained atom-trimer scattering results were related to the trimer relaxation rate constant that hopefully will be measured in the future experiments with ultracold mixtures of atoms and Efimov trimers.

The developed technique is applicable also to dimer-dimer scattering. Our first calculations confirm the nontrivial behavior of the dimer-dimer scattering length when approaching the unitary limit [4] but can provide results also at finite energies. Furthermore, the extension to fermionic systems in the unitary limit may have impact not only on the cold atom but also on nuclear physics, e.g., by clarifying to what extent four-nucleon resonances are universal.

The author thanks R. Lazauskas and L. Platter for discussions and suggestions.

- 
- [1] V. Efimov, Phys. Lett. B **33**, 563 (1970).
  - [2] E. Braaten and H.-W. Hammer, Phys. Rep. **428**, 259 (2006).
  - [3] H. W. Hammer and L. Platter, Eur. Phys. J. A **32**, 113 (2007).
  - [4] J. P. D’Incao, J. von Stecher, and C. H. Greene, Phys. Rev. Lett. **103**, 033004 (2009).
  - [5] J. von Stecher, J. P. D’Incao, and C. H. Greene, Nature Phys. **5**, 417 (2009).
  - [6] Y. Wang and B. D. Esry, Phys. Rev. Lett. **102**, 133201 (2009).
  - [7] T. Kraemer *et al*, Nature **440**, 315 (2006).
  - [8] F. Ferlaino *et al.*, Phys. Rev. Lett. **102**, 140401 (2009).
  - [9] L. Platter, H. W. Hammer, and U.-G. Meißner, Phys. Rev. A **70**, 052101 (2004).
  - [10] P. Grassberger and W. Sandhas, Nucl. Phys. **B2**, 181 (1967); E. O. Alt, P. Grassberger, and W. Sandhas, JINR report No. E4-6688 (1972).
  - [11] O. A. Yakubovsky, Yad. Fiz. **5**, 1312 (1967) [Sov. J. Nucl. Phys. **5**, 937 (1967)].
  - [12] A. Deltuva and A. C. Fonseca, Phys. Rev. C **75**, 014005 (2007).
  - [13] A. Deltuva and A. C. Fonseca, Phys. Rev. Lett. **98**, 162502 (2007); Phys. Rev. C **76**, 021001(R) (2007); Phys. Rev. C **81**, 054002 (2010).
  - [14] A. Deltuva, A. C. Fonseca, and P. U. Sauer, Phys. Lett. B **660**, 471 (2008).
  - [15] A. Deltuva and R. Lazauskas, Phys. Rev. A **82**, 012705 (2010).
  - [16] R. Lazauskas and J. Carbonell, Phys. Rev. A **73**, 062717 (2006).